A covalent S-F heterodimer of leucotoxin reveals molecular plasticity of β-barrel pore-forming toxins

Pierre Roblin, Valérie Guillet, Olivier R. Joubert, Daniel Keller, Monique Erard, Laurent Maveyraud, Gilles Prévost, Lionel Mourey

PROTEINS
STRUCTURE ■ FUNCTION ■ BIOINFORMATICS

A covalent S-F heterodimer of leucotoxin reveals molecular plasticity of β-barrel pore-forming toxins

Pierre Roblin,[1] Valérie Guillet,[1] Olivier Joubert,[2] Daniel Keller,[2] Monique Erard,[1] Laurent Maveyraud,[1] Gilles Prévost,[2] and Lionel Mourey[1]*

[1] Institut de Pharmacologie et de Biologie Structurale du CNRS et de l'Université Paul Sabatier (IPBS UMR 5089), F-31077 Toulouse, France

[2] Laboratoire de Physiopathologie et d'Antibiologie Microbiennes (EA 3432), Institut de Bactériologie de la Faculté de Médecine, Hôpitaux Universitaires de Strasbourg, F-67000 Strasbourg, France

ABSTRACT

Staphylococcal leucotoxins, leucocidins, and γ-hemolysins are bicomponent β-barrel pore-forming toxins (β-PFTs). Their production is associated with several clinical diseases. They have cytotoxic activity due to the synergistic action of a class S component and a class F component, which are secreted as water-soluble monomers and form hetero-oligomeric transmembrane pores, causing the lysis of susceptible cells. Structural information is currently available for the monomeric S and F proteins and the homoheptamer formed by the related α-hemolysin. These structures illustrate the start and end points in the mechanistic framework of β-PFT assembly. Only limited structural data exist for the intermediate stages, including hetero-oligomeric complexes of leucotoxins. We investigated the protein–protein interactions responsible for maintaining the final bipartite molecular architecture and describe here the high-resolution crystal structure and low-resolution solution structure of a site-specific cross-linked heterodimer of γ-hemolysin (HlgA T28C–HlgB N156C), which were solved by X-ray crystallography and small angle X-ray scattering, respectively. These structures reveal a molecular plasticity of β-PFTs, which may facilitate the transition from membrane-bound monomers to heterodimers.

Proteins 2008; 71:485–496.

***Key words:** pore-forming toxins; β-barrel; protein–protein interaction; molecular plasticity; covalent complex.*

INTRODUCTION

Staphylococcal leucotoxins (leucocidins and γ-hemolysins) constitute a subgroup of the β-barrel pore-forming toxin (β-PFT) family.[1] Leucotoxin-producing strains are associated with several clinical diseases, including pyodermatitis and bullous impetigo, respiratory tract infections, pneumonia, and antibiotic-associated diarrhea.[2] Furthermore, the presence of Panton-Valentine leucocidin (PVL) is strongly associated with infections due to community-associated methicillin-resistant *Staphylococcus aureus* strains[3] and it has recently been suggested that PVL may play a key role in pulmonary infections,[4,5] despite not being the major determinant of the diseases caused by these strains.[6] The biological activity of leucotoxins results from the synergistic action of two different proteins, S and F (≈32 and 34 kDa, respectively). S and F proteins are released as soluble monomers, which interact sequentially at the surface of monocytes, macrophages, polymorphonuclear neutrophils (PMNs), and erythrocytes to form inactive oligomeric prepores that ultimately develop into lytic transmembrane pores.[7,8]

Bicomponent leucotoxins are closely related to α-hemolysin (or α-toxin, 33 kDa), which oligomerizes to form a well characterized homoheptamer,[9] the crystal structure of which has provided the first high-resolution three-dimensional view of the architecture of an assembled β-PFT.[10] Each subunit of the α-hemolysin heptamer has three domains—the rim, β-sandwich, and stem domains—with the stem domain folding as a β-hairpin, which is involved in forming the transmembrane β-barrel pore. In contrast, the crystal structure of HlgB,[11] the class F component of γ-hemolysin, and those of the F and S proteins of PVL[12,13] exemplified the monomeric

The Supplementary Material referred to in this article can be found online at http://www.interscience.wiley.com/jpages/0887-3585/suppmat/.

Pierre Roblin and Valérie Guillet contributed equally to this work.

Grant sponsors: Access to EMBL/DESY was supported by the EU-13 access grant from the EU Research Infrastructure Action under the FP6 "Structuring the European Research Area Program" (contract No. RII3/CT/2004/5060008) and by the EMBL-Hamburg Strategy Fund. This work was supported by the Centre National de la Recherche Scientifique (UMR 5089), by the Direction de la Recherche et des Etudes Doctorales (EA 3432), and by funds from the Fondo Progetti of Provincia Autonoma di Trento (Project StaWars, EA 3432).

*Correspondence to: Lionel Mourey, IPBS-CNRS, 205 route de Narbonne, 31077 Toulouse Cedex, France. E-mail: lionel.mourey@ipbs.fr

Received 13 July 2007; Revised 21 September 2007; Accepted 1 October 2007
Published online 23 January 2008 in Wiley InterScience (www.interscience.wiley.com).
DOI: 10.1002/prot.21900

structure of staphylococcal β-PFTs, in which the stem domain folds against the protein core, and must therefore flip out and refold during pore assembly. Both the stoichiometry and arrangement of the F and S proteins within the leucotoxin pore have long been a matter of debate.[14–18] An octameric organization, with an alternating arrangement of F and S subunits in 1:1 stoichiometry has been clearly demonstrated for HlgB and HlgC (one of the two class S components of γ-hemolysin) based on the chemical cross-linking of cysteine mutants and genetic ligation, resulting in an F-S concatenated dimer.[19]

The structure of leucotoxin assemblies has yet to be solved. The difficulties involved include the absence of formation of any leucotoxin hetero-oligomers in the absence of membranes.[7,18] Thus, structural studies on the heterodimers constituting the minimal functional units necessary for construction of the leucotoxin pore may provide information about interprotomer interfaces and clues to the pathway to the prepore, a key issue for assembly. In a previous study, we engineered cysteine mutants of HlgB and HlgA (the second S component of γ-hemolysin), to generate a set of heterodimers linked by disulfide bridges. These covalently linked heterodimers were also found to form octamers[20] with an alternating arrangement of F and S subunits.[8] We report here the full structural characterization of the most active species identified. HlgA T28C–HlgB N156C, which has functional characteristics similar to those of the wild-type HlgA-HlgB toxin, has been crystallized, and its three-dimensional structure solved to a resolution of 2.4 Å. The solution structure of the heterodimeric complex was also studied at low resolution, using small-angle X-ray scattering (SAXS) experiments. We analyzed both structures and considered their role in the assembly of pore-forming leucotoxins.

MATERIAL AND METHODS

Production and biochemical characterization of the S-F covalent heterodimer

The disulfide-linked γ-hemolysin heterodimer was prepared from variants HlgA T28C and HlgB N156C, as previously described.[20] Both variants were produced as GST (glutathione S-transferase) fusion proteins in *Escherichia coli* BL21. They were purified by FPLC, using glutathione-affinity chromatography followed, after removal of the GST tag, by either cationic exchange (HlgA) or hydrophobic interaction (HlgB) chromatography. An octapeptide (Gly-Pro-Leu-Gly-Ser-Pro-Glu-Phe) was added to the N-terminus of each sequence, resulting in a theoretical molecular weight of 67700.7 Da. The HlgA T28C–HlgB N156C dimer was synthesized in the presence of 2,2′-dithiodipyridine and purified by hydrophobic interaction and cation-exchange chromatography to remove free HlgA T28C and HlgB N156C, respectively. Protein purity and stability were checked by SDS-PAGE and immunoblotting. The molecular integrity of covalent heterodimers was checked, as follows, after binding to PMNs. Human PMNs were prepared as described[20] and resuspended in 10 m*M* Hepes, 140 m*M* NaCl, 5 m*M* KCl, 10 m*M* glucose, and 0.1 m*M* EGTA, pH 7.3, at 5×10^7 cells/mL. The cells were incubated for 30 min at 22°C with 100 n*M* of pure heterodimer in the presence of 10 μL/mL antiprotease cocktail (Sigma) and 0.3 m*M* H_2O_2. The cells were washed thrice during 2 min at 800*g* at 22°C and then resuspended in the same buffer containing the antiprotease cocktail. The cells were transferred in MagNa Lyser Green Beads (Roche) and ground for 10 s at speed 6.0 in a FastPrep® Instrument (MP Biomedicals). The cell membranes were pelleted by ultracentrifugation at 30,000*g* for 20 min at 6°C. The membrane pellets were resuspended in 100 μL PBS, 1 m*M* EGTA, containing 1% (w/v) saponin (Sigma) and 20 μL/mL of the antiprotease cocktail, incubated for 10 min at 30°C and then centrifuged at 30,000*g* for 30 min at 6°C. The supernatants were mixed with an equal volume of denaturing buffer containing 100 m*M* Tris-HCl, 4% (w/v) SDS, 0.001% (w/v) Bromophenol Blue, and 15% (v/v) glycerol, pH 7.5. The samples were electrophoresed through the NuPAGE® 10% Bis-Tris gel system (Invitrogen), using Manufacturer's recommendations, and transferred onto 0.22 μm nitrocellulose membranes (Schleicher and Schuell) in 25 m*M* Bicine, 25 m*M* Bis-Tris, 1 m*M* EDTA, and 10% (v/v) methanol, pH 7.2. The leucotoxin complexes were immublotted with anti-HlgA and anti-HlgB affinity-purified rabbit polyclonal antibodies (1:2000 dilution). After incubation with horseradish peroxidase-conjugated secondary antibody, the blots were developed using Amersham ECL (GE Healthcare).

Crystallographic study

Dynamic light scattering studies were carried out in various buffers, with various heterodimer concentrations, to optimize the conditions for a unimodal distribution with good monodispersity. Scattered intensities were recorded at 293 K using a DynaPro-MS/X molecular-sizing instrument equipped with a microsampler (Protein Solutions). Then, the covalent complex was concentrated to 9 mg/mL in 50 m*M* MES-NaOH, 50 m*M* NaCl, pH 6.5. Crystallization was performed at 285 K, by vapor equilibration, using the hanging-drop method. Basic, extension, and low ionic screens (Sigma) were used for initial screening. Needle- and rod-shaped crystals suitable for diffraction studies were obtained in drops prepared by mixing two volumes of protein and one volume of reservoir solution containing 10% polyethylene glycol 8000, 0.05 *M* sodium citrate, pH 5.5; reservoir volumes of 500 μL were used. Diffraction data were collected at beamline ID14–2 of the European Synchrotron Radiation Facility (ESRF, Grenoble, France), with a wavelength set

at 0.933 Å using an ADSC Quantum 4R CCD detector. A complete set of diffraction data was collected at 2.4 Å using a single crystal, ($200 \times 50 \times 50$ μm^3) previously cryocooled in a stream of nitrogen gas at 100 K after immersion for 3 min in the crystallization solution supplemented with 20% (v/v) glycerol, and stored in liquid nitrogen. This crystal belonged to space group $P6_1$ with cell parameters $a = b = 140.0$, $c = 73.1$ Å, and one heterodimer per asymmetric unit. Matthews coefficient (V_m) and solvent content were 3.1 Å^3 Da^{-1} and 61%, respectively. All crystallographic calculations were carried out with the CCP4 suite,[21] using the graphical user interface.[22] X-ray diffraction data were processed with MOSFLM[23] and scaled with SCALA.[24] The structure of HlgA T28C–HlgB N156C was solved by molecular replacement with either Phaser[25] or MOLREP.[26] The search models corresponded to the coordinates of the previously solved crystal structures of HlgB (PDB code 1LKF[11]) and of the PVL S component (PDB code 1T5R[13]) truncated as polyalanines. Molecular replacement calculations led to a clear solution, making it possible to position the two search models in the unit cell with no crystal packing clash. Restrained refinement was performed with REFMAC[27] using a bulk solvent correction based on the Babinet principle and minimizing a maximum likelihood target function. After one round of refinement, the crystallographic R/R_{free} factors decreased from 0.496/0.504 to 0.405/0.470, for all data between 30.0 and 2.4 Å resolution. The resulting electron density map displayed blobs that unambiguously accounted for a disulfide link between the two molecules. Backbone modifications, side chains, and solvent molecules, added as neutral oxygen atoms when they appeared as positive peaks above 4.0σ and displayed acceptable hydrogen-bonding geometry, were introduced gradually, leading to final R and R_{free} values of 0.179 and 0.239, respectively. The refined model included 546 of the 595 amino acids found in the heterodimer construction. All residues belong to the allowed regions of a Ramachandran plot and 88.6% were in the most favored region. The 49 missing residues had either poorly defined or no electron density. They belong to loops of the rim domain for both HlgA and HlgB, the crossover connection of the stem domain of HlgB and the N-terminus of HlgA. The tendency of these regions to display disorder was noted in previous structural investigations on individual S and F components. The 34-residue side chains with little or no electron density were truncated to the last visible atom. A total of 173 water molecules were positioned in the electron density map.

Small-angle X-ray scattering experiments and data analysis

The synchrotron radiation X-ray scattering data were collected with the X33 camera[28,29] at the European Molecular Biology Laboratory (EMBL), on storage ring DORIS III of the Deutsches Elektronen Synchrotron (DESY) using a marresearch mar345 image plate detector. The scattering patterns from the γ-hemolysin HlgA T28C–HlgB N156C heterodimer were measured at several solute concentrations between 1.0 and 25 mg/mL and in 50 mM MES-NaOH, 50 mM NaCl, pH 6.5 in the presence of free radical scavengers. The data were collected at 12°C at a sample-detector distance of 2.7 m covering the momentum transfer range $0.10 < s < 4.5$ nm^{-1} ($s = 4\pi\sin\theta/\lambda$, where 2θ is the scattering angle and $\lambda = 1.5$ Å the X-ray wavelength). Data were collected over a period of 2–5 min. They were radially averaged by Mar-Primus (Konarev and Svergun, in preparation) and all subsequent data processing, analysis and modeling steps were carried out with PRIMUS,[30] and other programs of the ATSAS suite.[31] Difference curves after the subtraction of buffer scattering were scaled for protein concentration and extrapolated to infinite dilution to yield the final processed scattering curve.

The maximum dimension D_{max} of the heterodimer was estimated from the experimental data, using the orthogonal expansion program ORTOGNOM.[32] Forward scattering $I(0)$ and the radius of gyration R_g were evaluated using the Guinier approximation,[33] assuming that at very small angles ($s < 1.3/R_g$), intensity may be represented as $I(s) = I(0)\exp(-(sR_g)^2/3)$. These parameters were also calculated from the entire scattering pattern using the indirect transform package GNOM,[34] which also provides the distance distribution function $p(r)$ of the particle. The molecular mass of the solute was determined by comparing forward scattering with that for a reference solution of bovine serum albumin (MM = 66 kDa) prepared in 50 mM HEPES pH 7.5.

Scattering from the crystallographic model of the γ-hemolysin heterodimer was calculated using CRYSOL.[35] The atomic coordinates are input into the program, which then fits the experimental intensity $I(s)$ by adjusting the excluded volume of the particle and the contrast of the hydration layer surrounding the particle in solution to minimize discrepancy:

$$\chi^2 = \frac{1}{N-1}\sum_j \left[\frac{I_{exp}(s_j) - cI_{calc}(s_j)}{\sigma(s_j)}\right]^2 \qquad (1)$$

where N is the number of experimental points, $I_{exp}(s)$, $I_{calc}(s)$, and $\sigma(s_j)$ are the experimental and calculated intensity and the experimental error at the momentum transfer s_j, respectively, and c is a scaling factor. A low-resolution model of the γ-hemolysin heterodimer was generated *ab initio*, using the dummy atom model method, as implemented in the program DAMMIN,[36] which uses simulated annealing to search for a compact model that fits the experimental data to minimize the discrepancy in Eq. (1). We used SASREF[37] for rigid-body modeling of the heterodimeric complex against the exper-

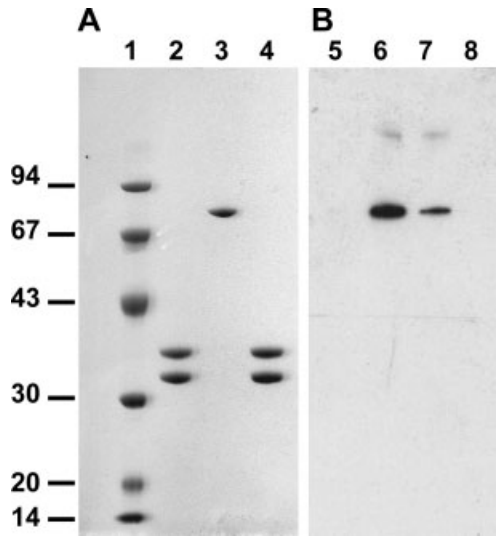

Figure 1

*Analysis of the purified HlgA T28C-HlgB N156C γ-hemolysin heterodimer. (**A**) SDS-PAGE and Coomassie blue staining of: lane 1, molecular weight ladder; lane 2, wild-type HlgA (32 kDa) and HlgB (34 kDa); lanes 3 and 4, HlgA T28C-HlgB N156C in nonreducing and reducing (20 mM DTT) conditions, respectively. (**B**) Immunoblotting after SDS-PAGE analysis of: lane 5, PMNs only; lane 6, HlgA T28C-HlgB N156C only; lanes 7 and 8, fractions retrieved after treatment of PMNs with HlgA T28C-HlgB N156C and extraction in the presence and absence of saponin, respectively.*

imental scattering data. The two subunits of the complex were treated as separate bodies and rigid-body modeling was restrained by the distance corresponding to the disulfide link between the two engineered cysteine residues.

Production of the figures

Figures 2, 3(A), 4, and 5(B) were produced with PyMol [DeLano W.L. The PyMOL molecular graphics system (2002) DeLano Scientific, San Carlos, CA]. Figure 3(B) was produced with ESPript.[38] STRIDE[39] was used for all secondary structure assignments.

Accession code

The coordinates and structure factors of the HlgA T28C–HlgB N156C complex have been deposited at the RCSB Protein Data Bank under the accession code 2QK7.

RESULTS

Crystal structure of an active leucotoxin covalent heterodimer

Despite the need for a complex preparation protocol, including several purification steps and thiol-protection/activation, quantitative yields of the pure HlgA T28C–HlgB N156C heterodimer were obtained. The purified heterodimer could be stored without degradation for several months at 4°C, as shown by SDS-PAGE in nonreducing conditions, which gave a single major band [Fig. 1(A)]. The HlgA T28C–HlgB N156C dimer had biological activity in cells, such as PMNs, similar to that of the wild-type HlgA-HlgB toxin.[20] We also checked that the macromolecular species recovered after insertion into PMN membranes and saponin treatment corresponded to intact dimers [Fig. 1(B)]. We crystallized the complex and solved the structure by molecular replacement using the structures of LukS-PV and HlgB (PDB accession codes 1T5R and 1LKF). Details of the structure determinations are provided in Table I.

The heterodimer consists of the γ-hemolysin proteins HlgA and HlgB covalently linked by a disulfide bridge between engineered cysteine residues (positions 28 and 156, respectively) [Fig. 2(A)]. Each protein is ellipsoid in form and can be divided into the typical β-sandwich, rim, and folded stem domains [Fig. 2(B)], with this fold

Table I

Statistics for Crystallographic Data Collection and Refinement

Data collection[a]	
Resolution range (Å)	30–2.40 (2.53–2.40)
Number of measured reflections	223,435 (30,919)
Number of unique reflections	32,122 (4659)
Completeness (%)	100 (100)
R_{sym} (%)	7.8 (31.8)
$I/\sigma I$	8.0 (2.3)
B_{Wilson} (Å^2)	39.5
Refinement[a]	
Resolution range (Å)	30–2.40 (2.46–2.40)
Number of reflections work/test	30,458/1625 (2222/127)
R factor	0.179 (0.207)
R_{free}	0.239 (0.288)
Refined model	
Number of observed residues/expected[b]	
HlgA T28C	259/288
HlgB N156C	287/307
Total	546/595
Missing residues	
HlgA T28C	Tag, 1–10, 64–68, 167–168, 242–243, 279–280
HlgB N156C	Tag, 1–2, 129–135, 198–200
Number of incomplete side chains	
HlgA T28C	25
HlgB N156C	9
Number of protein atoms	4303
Number of water molecules	173
Average B values (Å^2)	
Overall	47.3
Main chain	46.5
Side chain	47.8
Solvent	50.8
RMSD from ideal geometry	
Bond lengths (Å)	0.024
Bond angles (deg)	2.028
Planarity (Å)	0.009

[a]Numbers in parentheses are for the highest resolution shell.
[b]Taking into account the changes made to the sequence (see text).

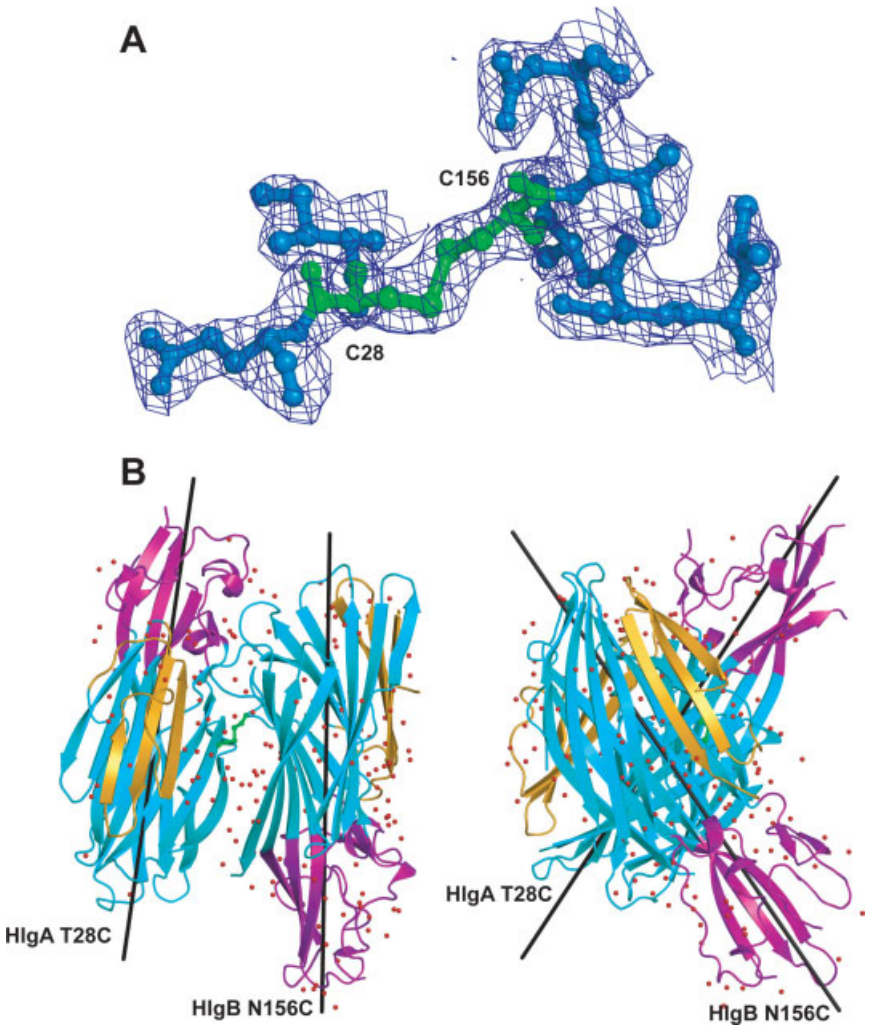

Figure 2

*Overall structure of the covalent HlgA T28C-HlgB N156C γ-hemolysin heterodimer. (**A**) Final 2mFo-DFc electron density map contoured at 1.0σ centered on the disulfide bridge linking residues Cys28 of HlgA and Cys156 of HlgB (in green). (**B**) Two perpendicular views of the heterodimer. HlgA T28C and HlgB N156C in ribbon representation, with the β-sandwich, rim and stem domains shown in cyan, magenta and orange, respectively. Solvent molecules are shown as red spheres and the major inertia axes as black lines.*

conserved in all individual leucotoxin S and F components.[1] Three long β-strands (from 15 to 20 residues) forming a spine are found to contribute to both the β-sandwich and rim domains. Over two-thirds of the ellipsoid, this spine forms part of one of the two facing antiparallel β-sheets (containing five to six strands) making up the β-sandwich domain, against which the three-stranded antiparallel β-sheet and the crossover connection found in the folded stem domain are stacked. The β-sheet of the sandwich domain that makes contact with the stem domain will be referred hereafter as the "internal" sheet. Conversely, the other β-sheet of the sandwich domain, which does not come into contact with the stem domain, will be referred to as the "external" sheet. In the remaining third of the ellipsoid, the spine is involved in the antiparallel β-sheet (containing three to four strands) defining the rim open-face sandwich. This β-sheet is topped by helical segments and loops in addition to two short β-strands. In the complex, the major inertia axes of HlgA and HlgB, corresponding to the longest axes of the ellipsoids, were found to intersect at an angle of 111°, leading to an almost perpendicular arrangement of the two proteins [Fig. 2(B)]. Cys28 is located at the N-terminus of the second β-strand of the internal β-sheet of HlgA and Cys156 occurs in a short extended loop (residues 154–160) between the first two β-strands of the external β-sheet of HlgB (Supplementary Fig. S1).

Investigations of the structure of the F and S monomeric components of PVL indicated that MES [2-(*N*-morpholino)-ethanesulfonic acid] was a suitable buffer

for manipulating and crystallizing proteins of this type. Further, two MES-binding sites were found in the rim domain of LukF-PV.[40] One of the MES molecules binding to these sites appears in the same position as a molecule of dipropanoyl phosphatidyl-choline in the complex formed with HlgB, providing clues concerning the possible mechanism of interaction of the rim domain with the lipid head groups of membranes.[11] In contrast, no such binding site was observed in the structure of LukS-PV, due to both sequence and structure variations in the rim domain.[13] Although HlgA T28C–HlgB N156C was crystallized in the presence of MES buffer, no clearly interpretable MES-binding site was found on the two subunits of the complex on close examination of the electron density map.

The structure of HlgA T28C provides the complete conformation of the β-PFT folded stem

We present here the first structural information for an S component of γ-hemolysin. The structure of HlgA T28C closely resembles that of monomeric LukS-PV, with a root-mean-square deviation (RMSD) value of 1.0 Å for 248 common Cα atoms covering all three domains [Supplementary Fig. S1(A)]. For comparison, the superimposition of the structures of HlgB in the monomeric form and in the covalent complex leads to an RMSD of 1.0 Å for 287 Cα atoms. In that case, deviations greater than the RMSD value are observed in connecting loops between β strands of the sandwich domain (residues 11–16, 44–49, and 232–235) and of the rim domain (residues 64–74, 186–187, 201–204, and 255–262). The largest deviations occur in two stretches of the HlgB polypeptide (residues 89–93 and 154–156 of the sandwich domain) contributing to the interface of the heterodimer [Supplementary Fig. S1(B)]. Excluding all these segments, the superposition gives an RMSD value of 0.6 Å for 236 Cα atoms.

The structure of HlgA T28C in the heterodimeric complex provides the first complete structural information about the conformation of the folded stem domain of leucotoxins. Indeed, poorly defined electron densities have impeded complete assignment of the folded stem in previously determined crystal structures of individual S and F components. Missing residues, ^{133}NGS^{135} in LukF-PV, ^{121}PSTGGN^{126} in LukS-PV, ^{129}SGGLNGN^{135} in free HlgB, and HlgB N156C in the heterodimer, essentially belong to the right-handed crossover connection found between the second and third strand of the folded stem β-sheet. SDS-PAGE of protein stocks in reducing conditions gave two single protein bands corresponding to the two components of the heterodimer [Fig. 1(A)]. This excludes the possibility of cleavage in this region accounting for the lack of electron density in the crossover connection for HlgB N156C. In contrast, electron density in this area was very well defined for HlgA T28C [Fig. 3(A)]. The conformation and anchoring of the crossover connection is maintained by a set of nine hydrogen bonds involving residues Ser122, Ile123, Gly124, Ser126, Gly127, and Asn130 of the crossover, residues Lys108, Tyr111, Asn112, and Ile113 of the first strand of the stem β-sheet, and Ala120 of the second strand of the stem β-sheet. Five of the stabilizing interactions connect the crossover connection to the first strand of the stem β-sheet, three are internal to the crossover connection, and six are sequence-specific and therefore involve at least one side-chain donor/acceptor atom (Supplementary Table S1). The topology of the crossover connection was analyzed with PROMOTIF.[41] The ^{123}IGGS^{126} residues are involved in a type II β-turn, in which both the main-chain nitrogen atom and the side-chain oxygen atom of Ser126 are hydrogen bonded to the main-chain oxygen atom of Ile123. The main-chain oxygen atom of Ser126 is also hydrogen bonded to the NZ atom of Lys108 whereas the main-chain oxygen atom of Gly124 is hydrogen bonded to the OG atom of Ser122, highlighting the specific role played by serine residues in stabilizing the crossover connection of HlgA (Supplementary Table S1). The amino-acid sequence of the crossover connection was found to be the least conserved part of the stem domain of leucotoxins [Fig. 3(B)]. Interestingly, Ser122 seems to be conserved among S proteins whereas interactions involving Lys108 and Ser126 should be specific to HlgA.

Remodeling of protein–protein interface during leucotoxin assembly

The macromolecular interface found within the HlgA T28C(HlgB N156C γ-hemolysin heterodimer involves the internal β-sheet of the sandwich domain and the stem domain in HlgA and the external β-sheet of the sandwich domain in HlgB [Fig. 4(A)]. In this configuration, the disulfide link is peripheral rather than located at the center of the interface. The geometric, topological and contact characteristics of the interface were analyzed with Intervor,[42] which uses an interface model based on the Euclidean Voronoi diagram and the related α-complex.[43] Calculations were performed either with the protein alone (AB model) or including water molecules (ABW model). In the AB model, the subunit–subunit interface (or AB interface) involves 93 atoms from HlgA and 68 atoms from HlgB. The two proteins therefore do not make equal contributions, possibly due to the concavity of HlgB observed in this area [Fig. 4(A)]. The AB interface corresponds to a surface area of 950 Å^2. Despite the medium resolution of the crystal structure (2.4 Å), it was interesting to include crystallographic water molecules in the analysis. In the ABW model, 153 HlgA atoms and 114 HlgB atoms contributed to the interface, corresponding to a 66% overall increase with respect to the AB

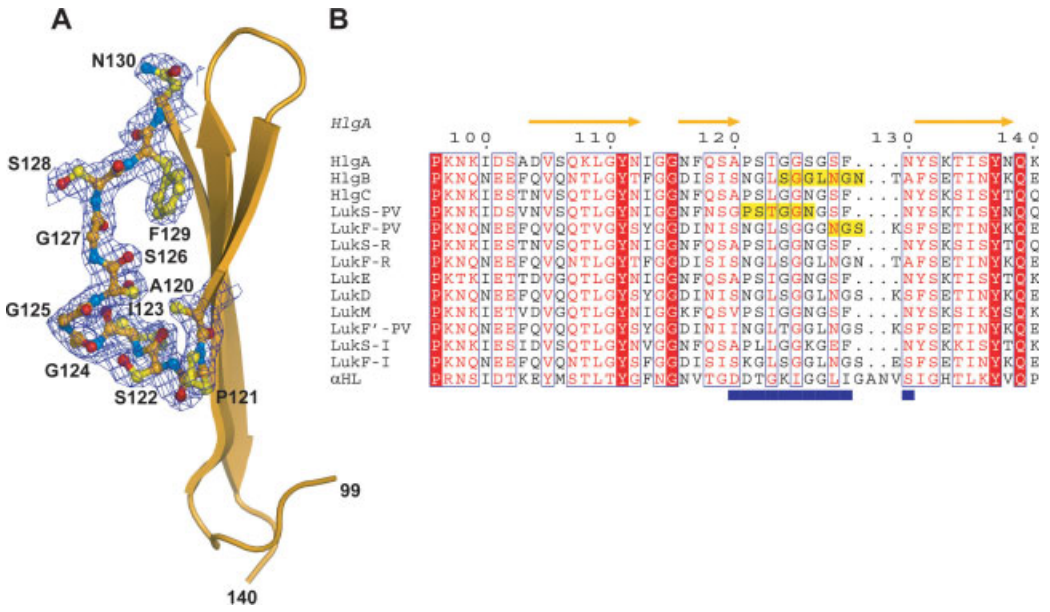

Figure 3

*Conformation of the stem domain of HlgA T28C. (**A**) Final 2mFo-DFc electron density map contoured at 1.0σ around residues delineating the crossover connection (ball-and-stick representation with main-chain carbon atoms in orange, side-chain carbons in yellow, oxygen in red and nitrogen in blue) of the stem domain (orange ribbon). (**B**) sequence alignment for the stem domain of leucotoxins and α-hemolysin. The S and F proteins of each leucotoxin were grouped. Sequence numbering is as for HlgA. Sequence similarities are highlighted in red, identical amino acids are indicated as white letters on a red background. Secondary structure elements (arrows for β-strands) of HlgA T28C are indicated at the top. Residues underlined in yellow are not defined in the corresponding crystal structures. The blue bar at the bottom delineates the residue range for which the density has been displayed.*

model, with 20 of the 173 water molecules involved in the interface. These water molecules have temperature factors similar to those of the interface protein atoms (average B factors of 49 and 44 Å^2, respectively). Taking all the patches, i.e. sets of Voronoi facets with edges in common,[43] of the subunit–subunit (AB) and subunit–solvent (A-W and B-W) interfaces together yielded a connected interface with a hole in the middle [Fig. 4(B)], with a surface area of 1220 Å^2. The concavity observed in the external β-sheet of the sandwich domain is conserved among all known leucotoxins and α-hemolysin structures. This concavity has no effect on the curvature of the interface [Fig. 4(A)], with a mean calculated value (4.3°) close to values reported for a test set of 96 protein–protein complexes taken from the protein data bank.[43] The dimer interface was then analyzed in terms of chemical properties, such as hydrogen bonding [Fig. 4(B)]. Nine direct hydrogen bonds, mostly involving side-chain atoms, and 19 bridging hydrogen bonds, mediated by seven water molecules and involving as many main-chain atoms as side-chain atoms, were identified (Supplementary Table S2).

SAXS measurements were undertaken to characterize the HlgA T28C–HlgB N156C covalent heterodimer in solution. Measurements were made at different protein concentrations, in the buffer used for crystallization. The rupture of disulfide bonds is the first site-specific radiation damage observed in proteins, and occurs even at cryogenic temperatures in the crystalline state.[44] Dithiothreitol (DTT) is the radical scavenger generally used to prevent radiation-induced degradation in synchrotron SAXS experiments. However, the disulfide-bridged heterodimer is sensitive to DTT, as shown by SDS-PAGE in reducing conditions (illustrated in Fig. 1). Therefore, protein solutions were analyzed in both the presence and absence of DTT. Alternatively, cryoprotectants such as glycerol and ethylene glycol were used, at a concentration of 5% (v/v). These organic molecules have been shown to reduce radiation damage in SAXS experiments.[45] Finally, two or three successive 2-, 3-, or 5-min exposure frames were collected and compared to check for possible radiation effects. Both radiation damage between successive frames and protein aggregation from the very first frame within a series were observed, whether or not a radical scavenger was used. Aggregation became more conspicuous with increasing protein concentration. A composite scattering curve was therefore obtained by merging data measured at three concentrations in the low- to medium-concentration range (2, 5, and 10 mg/mL), to minimize aggregation and to maximize the signal/noise ratio for the lower and higher values of momentum transfer, respectively [Fig. 5(A)]. The estimated

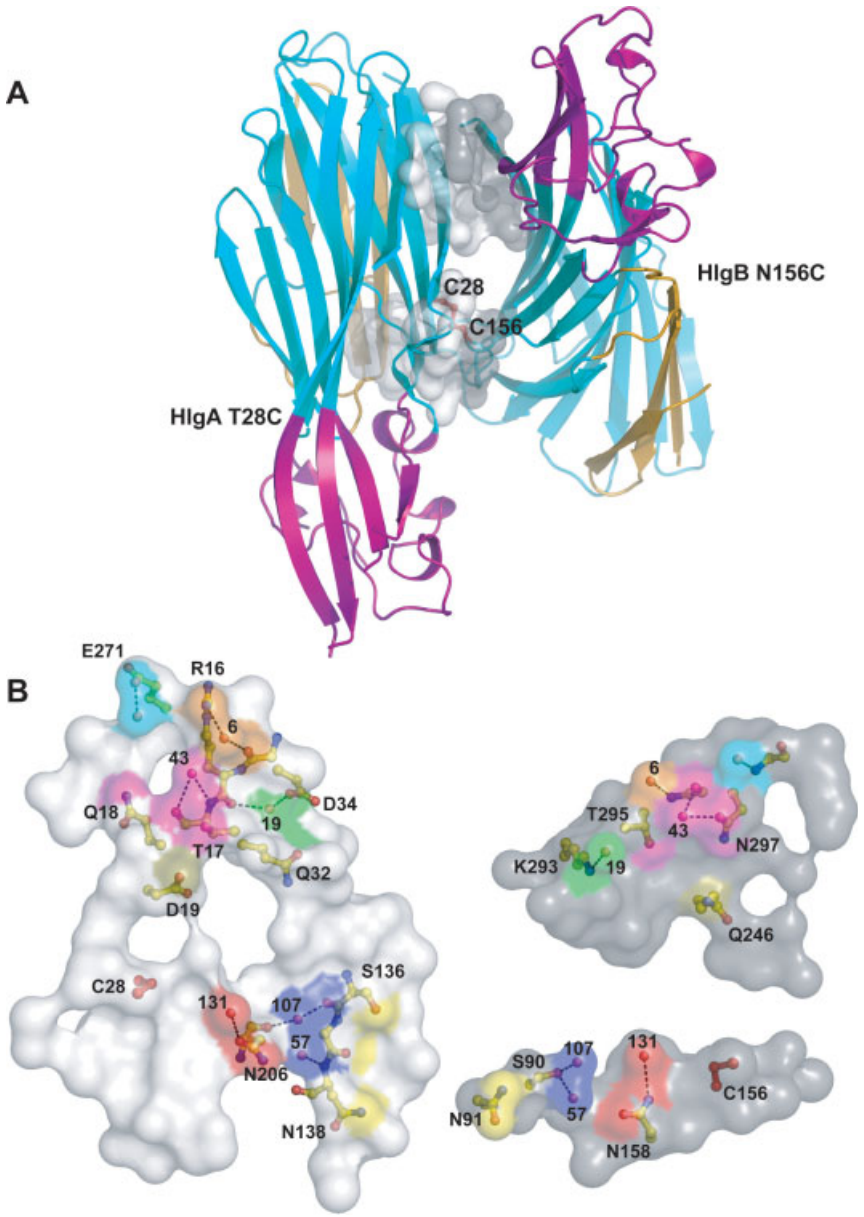

Figure 4

*Interface of the HlgA T28C–HlgB N156C γ-hemolysin heterodimer. (**A**) Side view of the molecular surface of interacting atoms in the AB model (HlgA T28C, white; HlgB N156C, gray). The two subunits are depicted as ribbon diagrams, using the same color scheme as in Figure 2. The disulfide bridge is shown in red. (**B**) Perpendicular views of the molecular surface of interacting atoms in the ABW model (HlgA T28C, left; HlgB N156C, right). The orientation in A has been rotated by ±90° around a vertical axis. Residues and water molecules involved in bridging hydrogen bonds are shown in ball-and-stick representation and as spheres, respectively (O, red; N, blue; C, yellow). The two cysteine residues are shown in red. For clarity, groups of inter-subunit interacting atoms are depicted using the same color on the molecular surfaces and bridging water molecules are duplicated on left and right views.*

molecular weight of the solute (59 ± 6 kDa) is consistent with the theoretical molecular weight (67.7 kDa), whereas the experimental radius of gyration obtained from the Guinier plot and distance distribution function $p(r)$ (29.7 and 29.5 Å, respectively) [inset, Fig. 5(A)] slightly exceed the value calculated based on the crystal structure (25.5 Å). This reflects aggregation problem even at low concentration. Accordingly, calculation of $p(r)$ was improved by using data truncated of the lowest values of momentum transfer leading to R_g = 26.7 Å and a decrease in D_{max} from 95 to 77 Å [inset, Fig. 5(A)]. The low-resolution shape of the γ-hemolysin heterodimer reconstructed *ab initio* fits the experimental data with χ = 0.9.

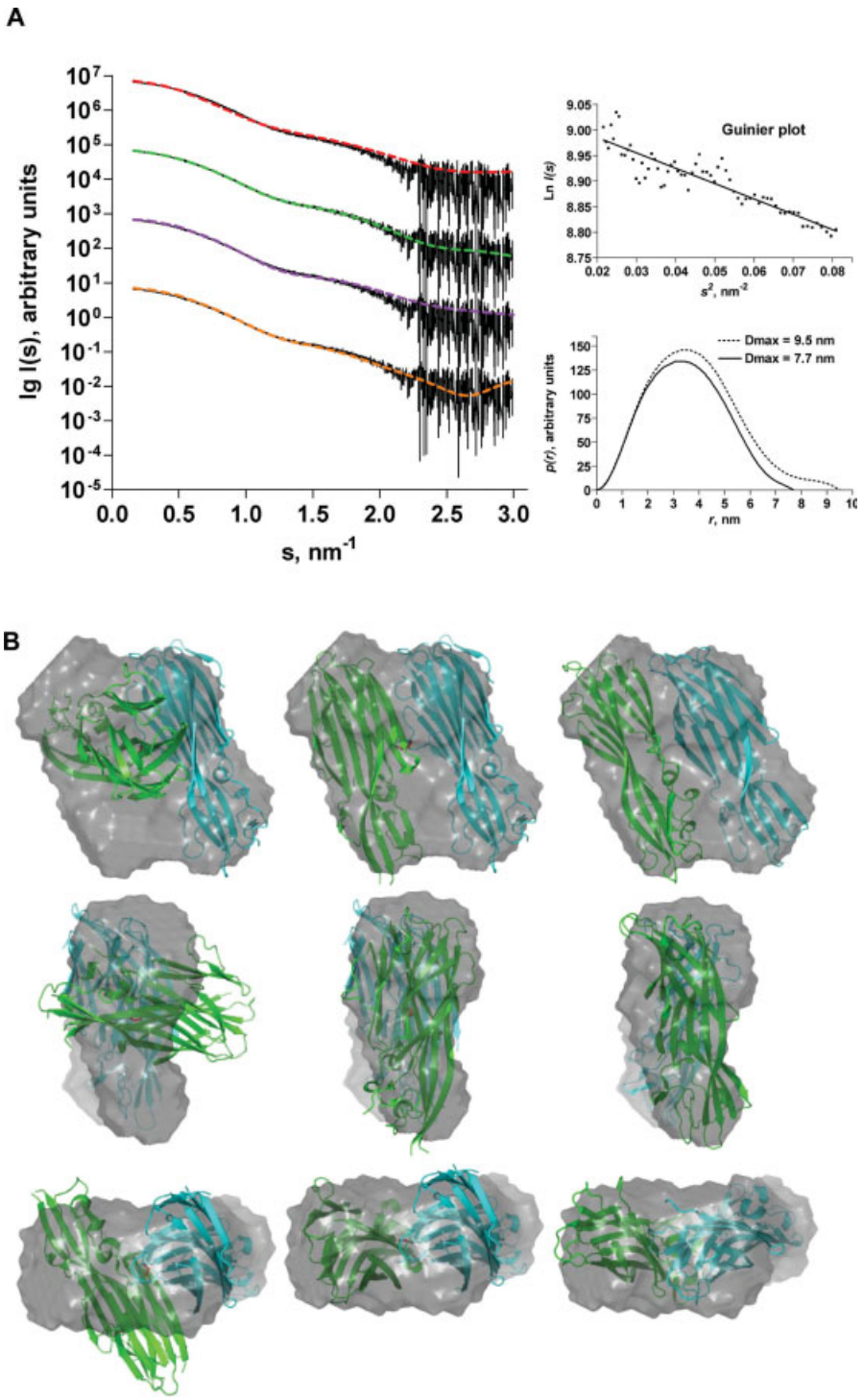

Figure 5

*SAXS analysis of the HlgA T28C-HlgB N156C γ-hemolysin heterodimer. (**A**) Experimental SAXS data from HlgA T28C-HlgB N156C and the scattering curves calculated from the different models described in the text. Dots with error bars show the experimental curve. Red lines show the scattering curve from the refined structure of HlgA T28C-HlgB N156C, orange lines show the scattering curve from the ab initio model, green and magenta lines show the calculated scattering from the SASREF model and the α-hemolysin pseudodimer, respectively. The logarithm of intensity is displayed as a function of momentum transfer $s = 4\pi\sin(\theta)/\lambda$, where 2θ is the scattering angle and $\lambda = 1.5$ Å is the X-ray wavelength. Each curve has been displaced downwards by 1 logarithmic unit for clarity. Inset, Guinier, and p(r) plots (see text). (**B**) Three perpendicular views of the ab initio model of HlgA T28C-HlgB N156C (semi-transparent surface) superimposed on the crystal structure (left column), the rigid model computed with SASREF (middle column), and the α-hemolysin pseudodimer (right column). The orientation on the top line has been rotated by 90° either along the vertical axis (middle line) or the horizontal axis (bottom line). Each subunit has a different color (HlgA T28C, green; HlgB N156C, blue). The side chains of the two cysteine residues are shown in red.*

The theoretical scattering pattern was calculated from the crystal structure, using CRYSOL, and compared with the experimental data. This pattern did not fit the experimental data well and displayed a systematic deviation χ value of 1.9 [Fig. 5(A)]. Consistent with these findings, the crystallographic model does not match the low-resolution shape model constructed *ab initio* with DAMMIN [Fig. 5(B)]. Indeed, it is obvious from the low-resolution envelope that the major axes of the two proteins of the complex in solution should be parallel rather than perpendicular as in the crystal structure. We then used SASREF for rigid-body modeling of the dimer against the SAXS data. The coordinates of HlgA T28C and HlgB N156C were taken separately and modeling was restrained by the distance corresponding to the disulfide link. The restored dimer obtained with SASREF fits the experimental data with a discrepancy value $\chi = 0.5$ and the level of agreement with the DAMMIN model is much higher, although not perfect [Fig. 5(B)]. Indeed, the tertiary structure of each leucotoxin component fit in the low-resolution molecular envelope; see, for example, the large lobe, which should correspond to the sandwich-stem part, allowing the unambiguous orientation of the high-resolution structure. The regions of the model that do not fit the envelope correspond to parts of the proteins for which structural data indicate mobility in leucotoxins[11–13]: the stem, the N-terminal part, and some of the loops of the rim domain. Finally, a α-hemolysin pseudodimer generated from the crystallographic coordinates of the heptamer, from which residues 1–16 and 104–151, respectively, corresponding to the amino-latch and to the unfolded stem domain were removed, did not fit better ($\chi = 1.3$) the SAXS data than the SASREF model (see Fig. 5).

DISCUSSION

As other β-PFTs, α-hemolysin, and leucotoxins are secreted as water-soluble monomeric proteins, which (upon binding to susceptible cells) undergo an assembly process that ultimately leads to the formation of transmembrane lytic pores. Convincing evidence has now been obtained that at least one leucotoxin, γ-hemolysin, forms octamers with a subunit stoichiometry of 1:1 and an alternating arrangement of F and S subunits.[8,20,46] Thus, formation of the γ-hemolysin octamer requires two types of subunit–subunit interface (S-F and F-S) whereas α-hemolysin and *Bacillus anthracis* protective antigen are single polypeptides β-PFTs producing well characterized homoheptamers.[9,47] The crystallographic structures of the water-soluble monomeric forms of leucotoxin F and S components have been solved.[11–13] It is generally accepted that these structures, together with that of α-hemolysin, represent the start and end points in β-PFT assembly.[11,40,48] In contrast, limited structural data are available for intermediate stages from membrane-bound monomers to the nonlytic prepore, and concerning the unfolding-refolding dynamics of the stem domain. As the formation of leucotoxin hetero-oligomers has not yet been shown to occur in solution,[7,18] we initiated a comprehensive study of the protein–protein interactions responsible for maintaining the final bipartite architecture of the (pre)pore. We designed and produced covalent heterodimers of γ-hemolysin consisting of HlgA and HlgB cysteine mutants linked by a disulfide bridge. Our reasoning for the choice of mutations was based on the important role played by Thr28 in the assembly of both γ-hemolysin[49] and PVL,[13] as previously reported for the equivalent residue (His35) in α-hemolysin.[50,51] Thus, Thr28 and its closest neighbor (Thr21) in HlgA, and residues of HlgB exposed to the solvent that may face the two threonine residues within the (pre)pore were replaced by cysteine residues and the resulting mutants were used for the preparation and testing of 20 covalent heterodimers.[20] The high- and low-resolution structures of the fully functional HlgA T28C–HlgB N156C heterodimer were determined by X-ray crystallography and SAXS, respectively.

We searched the entire PDB V3 (http://wwpdb-remediation.rutgers.edu/) for SSBOND records, excluding intra-chain disulfides, resulting in a list of all known structures of disulfide-mediated macromolecular assemblies. The resulting PDB subset had more than 1200 entries, with a high level of redundancy. Most of these structures correspond to hetero-oligomeric proteins, such as Fab and Fv fragments, hemagglutinin, and thrombin and other blood coagulation factors, insulin, chymotrypsin, venom toxins, type-II ribosome-inactivating proteins (RIP-II), and T-cell receptor. We found only a few examples of disulfide-mediated covalent bimolecular protein complexes. Besides cytochrome c peroxidase—cytochrome c complex,[52] the structure of HlgA T28C–HlgB N156C provides to our knowledge the second example of a specifically designed cross-linked protein-protein complex. The two subunits were found to be oriented almost at right angles in the crystal structure, an unexpected orientation for the assembled toxin. Indeed, the angle between the major axes of two successive subunits in the α-hemolysin heptamer is 21°. We then carefully examined the crystal packing of HlgA T28C–HlgB N156C, in which HlgA T28C displays four interfaces burying 64, 64, 119, and 331 Å^2 (for a total of 578 Å^2), corresponding to a loose environment. HlgB N156C has a more densely packed environment, with six interfaces burying 135, 282, 301, 337, 473, and 517 Å^2 (for a total of 2045 Å^2). Furthermore, two symmetry mates interact with both γ-hemolysin subunits, one of which makes direct contact with the rim domain of HlgB N156C whereas the other sits between the two β-sandwich domains (Supplementary Fig. S2). These interactions are obviously not compatible with the parallel alignment of HlgA T28C and

HlgB N156C in the crystal. However, we can draw no firm conclusions as to whether these favorable intermolecular contacts induced the observed shear effect during the crystallization process or whether crystal growth occurred owing to some preformed misalignment within the heterodimer. Further analysis using the "Protein interfaces, surfaces and assemblies service" PISA[53] at European Bioinformatics Institute (http://www.ebi.ac.uk/msd-srv/prot_int/pistart.html) confirmed that the conformation of HlgA T28C-HlgB N156C in the crystal does not correspond to a stable quaternary assembly. According to the SAXS results, a parallel orientation seems to prevail in solution. Moreover, rigid body fitting within the low-resolution envelope shows that the correct orientation of the two subunits, leading to the formation of a functional interface, may require not only a change in disulfide bridge dihedral angles, but also local rearrangements in the polypeptide segments bearing the cysteine residues. These results were corroborated by preliminary molecular mechanics calculations (data not shown).

With respect to the assembly of leucotoxin pores and, particularly, the transition between the intermediate stages mentioned above, the membrane-bound S and F subunits must diffuse on the membrane surface until they encounter appropriate partners. FRET measurements have shown that the specific formation of heterodimers on the membranes is promoted by side-by-side collisions, and it has been suggested that the structural changes occurring upon membrane binding may strengthen such interactions between subunits.[18] The labile interaction observed in the X-ray structure of the covalent heterodimer suggests there is some molecular plasticity, which might be physiologically relevant. This structure may thus provide a snapshot of the onset of the dynamic trajectory leading from stochastic encounters of monomeric F and S proteins to correctly aligned F-S heterodimers, which were also studied here by SAXS. Such heterodimers would then promote further oligomerization through cooperative dimer–dimer interactions.

ACKNOWLEDGMENTS

We thank the scientific staff of the European Synchrotron Radiation Facility (Grenoble, France) and EMBL/DESY (Hamburg, Germany) for the use of their excellent data collection facilities. We thank Dmitri Svergun and members of the EMBL X33 beamline for their help during SAXS experiments and for useful advice on the programs of the ATSAS package. We thank Frédéric Cazals for his precious help and comments about analysis of the dimer interface. We would also like to thank Dominique Durand for providing very helpful advice on SAXS analysis and Ralf Grosse-Kunstleve who carried out Protein Data Bank searches. We also acknowledge the very constructive remarks of one referee.

REFERENCES

1. Prévost G, Mourey L, Colin DA, Monteil H, Serra MD, Menestrina G. Alpha-helix and beta-barrel pore-forming toxins (leucocidins, alpha-, gamma- and delta-cytolysins) of *Staphylococcus aureus*. In: Alouf JE, Popoff MR, editors. The comprehensive sourcebook of bacterial protein toxins, 3rd ed. London: Academic Press; 2006. pp 588–605.
2. Prévost G, Menestrina G, Colin DA, Werner S, Bronner S, Serra MD, Moussa LB, Coraiola M, Gravet A, Monteil H. Staphylococcal bicomponent leucotoxins, mechanism of action, impact on cells and contribution to virulence. In: Menestrina G, Serra MD, Lazarovici P, editors. Pore-forming peptides and protein toxins. London: Taylor and Francis; 2003. pp 3–26.
3. Chambers HF. Community-associated MRSA-resistance and virulence converge. N Engl J Med 2005;352:1485–1487.
4. Gillet Y, Issartel B, Vanhems P, Fournet JC, Lina G, Bes M, Vandenesch F, Piémont Y, Brousse N, Floret D, Etienne J. Association between *Staphylococcus aureus* strains carrying gene for Panton-Valentine leukocidin and highly lethal necrotising pneumonia in young immunocompetent patients. Lancet 2002;359:753–759.
5. Labandeira-Rey M, Couzon F, Boisset S, Brown EL, Bes M, Benito Y, Barbu EM, Vazquez V, Hook M, Etienne J, Vandenesch F, Bowden MG. *Staphylococcus aureus* Panton-Valentine leukocidin causes necrotizing pneumonia. Science 2007;315:1130–1133.
6. Voyich JM, Otto M, Mathema B, Braughton KR, Whitney AR, Welty D, Long RD, Dorward DW, Gardner DJ, Lina G, Kreiswirth BN, DeLeo FR. Is Panton-Valentine leukocidin the major virulence determinant in community-associated methicillin-resistant *Staphylococcus aureus* disease? J Infect Dis 2006;194:1761–1770.
7. Miles G, Jayasinghe L, Bayley H. Assembly of the Bi-component leukocidin pore examined by truncation mutagenesis. J Biol Chem 2006;281:2205–2214.
8. Viero G, Cunaccia R, Prévost G, Werner S, Monteil H, Keller D, Joubert O, Menestrina G, Dalla Serra M. Homologous versus heterologous interactions in the bicomponent staphylococcal gamma-haemolysin pore. Biochem J 2006;394:217–225.
9. Gouaux JE, Braha O, Hobaugh MR, Song L, Cheley S, Shustak C, Bayley H. Subunit stoichiometry of staphylococcal alpha-hemolysin in crystals and on membranes: a heptameric transmembrane pore. Proc Natl Acad Sci USA 1994;91:12828–12831.
10. Song L, Hobaugh MR, Shustak C, Cheley S, Bayley H, Gouaux JE. Structure of staphylococcal alpha-hemolysin, a heptameric transmembrane pore. Science 1996;274:1859–1866.
11. Olson R, Nariya H, Yokota K, Kamio Y, Gouaux E. Crystal structure of staphylococcal LukF delineates conformational changes accompanying formation of a transmembrane channel. Nat Struct Biol 1999;6:134–140.
12. Pédelacq JD, Maveyraud L, Prévost G, Baba-Moussa L, Gonzalez A, Courcelle E, Shepard W, Monteil H, Samama JP, Mourey L. The structure of a *Staphylococcus aureus* leucocidin component (LukF-PV) reveals the fold of the water-soluble species of a family of transmembrane pore-forming toxins. Structure 1999;7:277–287.
13. Guillet V, Roblin P, Werner S, Coraiola M, Menestrina G, Monteil H, Prévost G, Mourey L. Crystal structure of leucotoxin S component: new insight into the Staphylococcal beta-barrel pore-forming toxins. J Biol Chem 2004;279:41028–41037.
14. Ferreras M, Hoper F, Dalla Serra M, Colin DA, Prévost G, Menestrina G. The interaction of *Staphylococcus aureus* bi-component gamma-hemolysins and leucocidins with cells and lipid membranes. Biochim Biophys Acta 1998;1414:108–126.
15. Sugawara N, Tomita T, Kamio Y. Assembly of *Staphylococcus aureus* gamma-hemolysin into a pore-forming ring-shaped complex on the surface of human erythrocytes. FEBS Lett 1997;410:333–337.
16. Sugawara-Tomita N, Tomita T, Kamio Y. Stochastic assembly of two-component staphylococcal gamma-hemolysin into heterohepta-

meric transmembrane pores with alternate subunit arrangements in ratios of 3:4 and 4:3. J Bacteriol 2002;184:4747–4756.
17. Miles G, Movileanu L, Bayley H. Subunit composition of a bicomponent toxin: staphylococcal leukocidin forms an octameric transmembrane pore. Protein Sci 2002;11:894–902.
18. Nguyen VT, Kamio Y, Higuchi H. Single-molecule imaging of cooperative assembly of gamma-hemolysin on erythrocyte membranes. EMBO J 2003;22:4968–4979.
19. Jayasinghe L, Bayley H. The leukocidin pore: evidence for an octamer with four LukF subunits and four LukS subunits alternating around a central axis. Protein Sci 2005;14:2550–2561.
20. Joubert O, Viero G, Keller D, Martinez E, Colin DA, Monteil H, Mourey L, Dalla Serra M, Prévost G. Engineered covalent leucotoxin heterodimers form functional pores: insights into S-F interactions. Biochem J 2006;396:381–389.
21. Collaborative Computational Project Number 4. The CCP4 suite: programs for protein crystallography. Acta Crystallogr Sect D 1994; 50:760–763.
22. Potterton E, Briggs P, Turkenburg M, Dodson E. A graphical user interface to the CCP4 program suite. Acta Crystallogr D Biol Crystallogr 2003;59:1131–1137.
23. Leslie AGW. Profile fitting. In: Helliwell JR, Machin PA, Papiz MZ, editors. Proceedings of the Daresbury study weekend: computational aspects of protein crystal data analysis. Warrington, UK: Science and Engineering Research Council, Daresbury Laboratory; 1987. pp 39–50.
24. Evans PR. Data reduction. In: Sawyer L, Isaacs N, Bailey S, editors. Proceedings of the CCP4 study weekend: data collection and processing. Warrington, UK: Science and Engineering Research Council, Daresbury Laboratory; 1993. pp 114–122.
25. Storoni LC, McCoy AJ, Read RJ. Likelihood-enhanced fast rotation functions. Acta Crystallogr D Biol Crystallogr 2004;60:432–438.
26. Vagin A, Teplyakov A. MOLREP: an automated program for molecular replacement. J Appl Crystallogr 1997;30:1022–1025.
27. Murshudov GN, Vagin AA, Dodson EJ. Refinement of macromolecular structures by the maximum-likelihood method. Acta Crystallogr Sect D Biol Crystallogr 1997;53:240–255.
28. Koch M, Bordas J. X-ray diffraction and scattering on disordered systems using synchrotron radiation. Nucl Instrum Methods 1983; 208:461–469.
29. Boulin C, Kempf R, Gabriel A, Koch M. Data acquisition systems for linear and area X-ray detectors using delay line readout. Nucl Instrum Methods Phys Res A 1988;269:312–320.
30. Konarev P, Volkov V, Sokolova A, Koch M, Svergun D. PRIMUS: a Windows PC-based system for small-angle scattering data analysis. J Appl Crystallogr 2003;36:1277–1282.
31. Konarev PV, Petoukhov MV, Volkov VV, Svergun DI. ATSAS 2.1, a program package for small-angle scattering data analysis. J Appl Crystallogr 2006;39:277–286.
32. Svergun D. A direct indirect method of small-angle scattering data treatment. J Appl Crystallogr 1993;26:258–267.
33. Guinier A. La diffraction des rayons X aux très petits angles: application à l'étude de phénomènes ultramicroscopiques. Ann Phys (Paris) 1939;12:161–237.
34. Svergun D. Determination of the regularization parameter in indirect-transform methods using perceptual criteria. J Appl Crystallogr 1992;25:495–503.
35. Svergun D, Barberato C, Koch M. CRYSOL—a program to evaluate X-ray solution scattering of biological macromolecules from atomic coordinates. J Appl Crystallogr 1995;28:768–773.
36. Svergun DI. Restoring low resolution structure of biological macromolecules from solution scattering using simulated annealing. Biophys J 1999;76:2879–2886.
37. Petoukhov M, Svergun D. Global rigid body modeling of macromolecular complexes against small-angle scattering data. Biophys J 2005; 89:1237–1250.
38. Gouet P, Courcelle E, Stuart D, Metoz F. ESPript: multiple sequence alignments in PostScript. Bioinformatics 1998;15:305–308.
39. Frishman D, Argos P. Knowledge-based protein secondary structure assignment. Proteins 1995;23:566–579.
40. Prévost G, Mourey L, Colin DA, Menestrina G. Staphylococcal pore-forming toxins. Curr Top Microbiol Immunol 2001;257:53–83.
41. Hutchinson EG, Thornton JM. PROMOTIF–a program to identify and analyze structural motifs in proteins. Protein Sci 1996;5:212–220.
42. Cazals F. Geometric, topological and contact analysis of interfaces in macro-molecular complexes: from the atomic scale to the complex scale using Intervor. INRIA Res Rep 2006; Report No. 5864.
43. Cazals F, Proust F, Bahadur RP, Janin J. Revisiting the Voronoi description of protein-protein interfaces. Protein Sci 2006;15:2082–2092.
44. Garman EF, McSweeney SM. Progress in research into radiation damage in cryo-cooled macromolecular crystals. J Synchrotron Radiat 2007;14:1–3.
45. Kuwamoto S, Akiyama S, Fujisawa T. Radiation damage to a protein solution, detected by synchrotron X-ray small-angle scattering: dose-related considerations and suppression by cryoprotectants. J Synchrotron Radiat 2004;11:462–468.
46. Jayasinghe L, Miles G, Bayley H. Role of the amino latch of staphylococcal alpha-hemolysin in pore formation: a co-operative interaction between the N terminus and position 217. J Biol Chem 2006; 281:2195–2204.
47. Lacy DB, Wigelsworth DJ, Melnyk RA, Harrison SC, Collier RJ. Structure of heptameric protective antigen bound to an anthrax toxin receptor: a role for receptor in pH-dependent pore formation. Proc Natl Acad Sci USA 2004;101:13147–13151.
48. Gouaux E. Channel-forming toxins: tales of transformation. Curr Opin Struct Biol 1997;7:566–573.
49. Meunier O, Ferreras M, Supersac G, Hoeper F, Baba-Moussa L, Monteil H, Colin DA, Menestrina G, Prévost G. A predicted beta-sheet from class S components of staphylococcal gamma-hemolysin is essential for the secondary interaction of the class F component. Biochim Biophys Acta 1997;1326:275–286.
50. Jursch R, Hildebrand A, Hobom G, Tranum-Jensen J, Ward R, Kehoe M, Bhakdi S. Histidine residues near the N terminus of staphylococcal alpha-toxin as reporters of regions that are critical for oligomerization and pore formation. Infect Immun 1994;62: 2249–2256.
51. Krishnasastry M, Walker B, Braha O, Bayley H. Surface labeling of key residues during assembly of the transmembrane pore formed by staphylococcal alpha-hemolysin. FEBS Lett 1994;356:66–71.
52. Guo M, Bhaskar B, Li H, Barrows TP, Poulos TL. Crystal structure and characterization of a cytochrome c peroxidase-cytochrome c site-specific cross-link. Proc Natl Acad Sci USA 2004;101:5940–5945.
53. Krissinel E, Henrick K. Inference of macromolecular assemblies from crystalline state. J Mol Biol 2007;372:774–797.